Nat Hazards (2018) 92:1355–1369
https://doi.org/10.1007/s11069-018-3254-7

ORIGINAL PAPER

The present-day active deformation in the central and northern parts of the Gulf of Suez area, Egypt, from earthquake focal mechanism data

I. Abu El-Nader[1,2] · **H. M. Hussein**[1,2]

Received: 20 August 2017 / Accepted: 4 March 2018 / Published online: 16 March 2018

Abstract The average seismic strain rate is estimated for the seismotectonic zone of the northern/central parts of the Gulf of Suez. The principal strain rate tensor and velocity tensor were derived from a combination of earthquake focal mechanisms data and seismic moment of small-sized earthquakes covering a time span of 13 years (1992–2004). A total of 17 focal mechanism solutions have been used in the calculation of the moment tensor summation. The local magnitudes (MLs) of these events range from 2.8 to 4.7. The analysis indicates that the dominant mode of deformation in the central and northern parts of the Gulf of Suez is extension at a rate of 0.008 mm/year in N28°E direction and a small crustal thinning of 0.0034 mm/year. This low level of strain means that this zone experienced a little seismic deformation. There is also a right lateral shear motion along the ESE–WNW direction. This strain pattern is consistent with the predominant NW–SE normal faulting and ESE–WNW dextral transtensive faults in this zone. Comparing the results obtained from both stress and strain tensors, we find that the orientations of the principal axes of both tensors have the same direction with a small difference between them. Both tensors show a predominantly extensional domain. The nearly good correspondence between principal stress and strain orientations in the area suggests that the tectonic strength is relatively uniform for this crustal volume.

Keywords Focal mechanism · Strain tensor · Scaler seismic moment · Gulf of Suez · Velocity tensor · Principal strain rate tensor

✉ I. Abu El-Nader
ememan70@yahoo.com

[1] Seismology Department, National Research Institute of Astronomy and Geophysics, Helwan, Egypt

[2] North Africa Seismological Group for Earthquakes and Tsunami Studies, NAGET, Net40 OEA ICTP, Milan, Italy

1 Introduction

The Gulf of Suez is one of the most important and seismically active regions in Egypt. The area of study occupies its northern and central parts. The seismotectonic characteristics of this area are less studied and not fully understood compared to the southern part of the Gulf of Suez. There is no previous attempt for evaluating the strain field in this area. However, a first attempt for determining the state of stress in this area from the inversion of the focal mechanisms data was made by Abu El-Nader (2009) and Morsy et al. (2011). Their result showed that the northern part of the Gulf is subjected to NE–SW to NNE–SSW horizontal extensional stress. The present study is considered to be an extension of the previous work of Morsy et al. (2011) in the same zone. Their work focuses on the importance of the focal mechanism solutions in the determination of the regional stress in the northern/central parts of the Gulf of Suez. However, in the present paper we seek how the source mechanisms of earthquakes may control the style and direction of seismic strain pattern across this seismic region. This means estimating displacement from a combination of fault plane solutions and scalar seismic moments released from a number of earthquakes occurring in a given volume (Kostrov 1974). This provides a major constraint on seismotectonic reconstruction within a deforming region (Jackson and Mckenzie 1988; Ekstrom and England 1989; Amelung 1996). This will increase our understanding of the dynamic process in the crust.

It is well known that the Gulf of Suez is now the least active of the three branches which meet at the southern tip of Sinai Peninsula, in particular its northern part. Whether or not the northern part of the Gulf of Suez is still undergoing extension or inactive is under debate. Numerous investigators attempted to quantify the amount of extension at various locations along the rift using different approaches (e.g., geometric analysis, subsidence models or geophysical interpretation; see Patton et al. 1994; Bosworth 1995). They all confirm that there is a decrease in extension from south to north along the rift.

The Gulf of Suez is characterized by low to moderate seismic activity, except its southern part (e.g., Maamoun et al. 1984; Kulhanek et al. 1992; Hussein et al. 2006). The northern Gulf of Suez does not yield high-magnitude seismic activity compared to the southern part, northern Red Sea and Gulf of Aqaba (Fig. 1). This activity appears to be low rather than diffuse. On the other hand, Daggett et al. (1986) suggested that there is a lack of significant seismicity in the northern and central parts of the Gulf of Suez which we consider here as one of the seismic zones. The installation of Egyptian National Seismological Network (ENSN) showed that there is a considerable seismic activity in this zone. There is also a considerable amount of reliable focal mechanism solutions that provide new insights into the abundant neotectonic activity in this zone. The main purpose of this study is the calculation of the strain tenor. This is desired for a good understanding of the seismotectonic features of this zone. In this work, the reliable fault plane solutions of 17 events are used in order to perform a strain tensor analysis and estimate the active crustal deformation. Then we compare the estimated strain results with results obtained from the stress tensor (Morsy et al. 2011) and the results deduced from GPS measurements in previous studies (El-Fiky 2005; Abdel-Monem et al. 2011).

1.1 Geology and structural setting

The Gulf of Suez rift represents the northern extension of the Red Sea rift system (Said 1962), both open at N30°W, with a very low amount of extension directed to N60°E (Steckler et al. 1988; Younes and McClay 2002). It runs northwest, forming depression

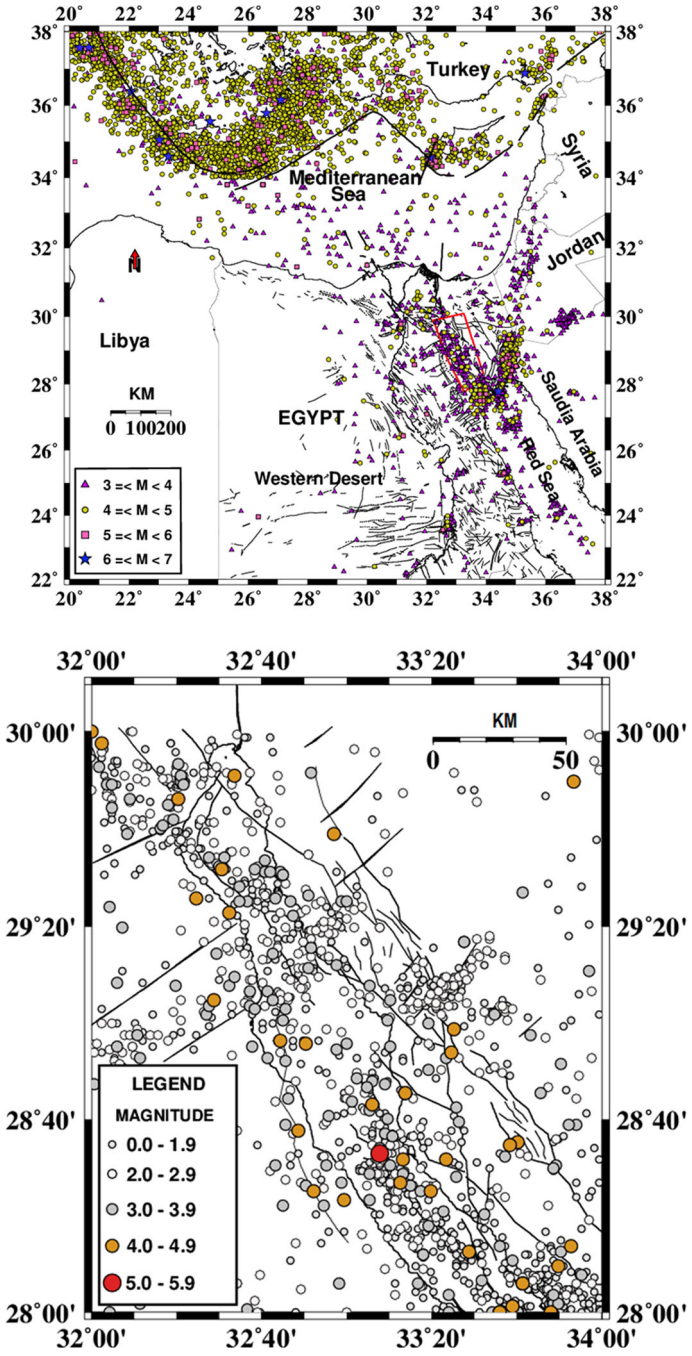

Fig. 1 At top, a map of earthquake activity in Egypt and surrounding area including the central/northern Gulf of Suez area (rectangular of red color) that appears at bottom showing the distribution of earthquake activity in combination with its structural setting. (Modified after Bosworth and McClay (2001) and Amer et al. (2012))

which is elongated about 300 km in length and 80 km in width. The water depth is only 40–60 m.

The Gulf of Suez rift consists of a three large scale half grabens of opposite tilt direction alternating along strike (the dip provinces of Moustafa 1976). The SW dipping half grabens distinguishes the northern and southern sectors of the Gulf. However, the central half graben reflects a dip toward the NE direction. Such changes in the tilt directions of adjacent half grabens (Moustafa 1995) are accompanied by a reversal in the dip of the detachment surfaces (Bosworth 1985). Therefore, the northern and southern dip provinces are dominated by faults that should dip to the NE, while the central part is dominated by faults that should dip to SW direction, a typical configuration of most active extensional basins. Each of the three extensional basins is delimited on one side by the major listric bounding normal faults and includes several fault blocks with internal planar extensional faults. These half grabens are linked along strike by two hinge zones oblique to the rift trend (Moustafa 1976).

The Gulf of Suez rift was developed through three tectonic subsidence and extensional phases. The first stage of rifting initiated in the late Oligocene to early Miocene. Such stage was governed by orthogonal rifting as a response to N60°E extension and the rift shoulders start to uplift and the subsidence rate of the pre rift succession was very weak. The second stage of rifting began during early to middle Miocene (active rifting stage), by increasing the extensional force in the NE direction. This phase of rapid tectonic subsidence corresponds to the main extension along the Gulf of Suez rift (Moretti and Colletta 1987). By middle Miocene, the direction of extension changed to become N40E (oblique extension). The oblique rifting phase led to the creation of a series of tilted fault blocks separated by the oblique slip accommodation zones. This phase was also accompanied by a compressional force-oriented N50 W that produced the left lateral Dead Sea Transform Fault System (Garfunkel and Ben-Avraham 1996; Lyberis 1988; McClusky et al. 2003). As a result, the extension in the Gulf of Suez rift rotated clockwise toward a perpendicular trend, which decreased the rate of opening to in the Gulf of Suez to < 1 mm/year (Steckler et al. 1988). Generally, there are four major populations of fault trends that defined the shapes of the present rift blocks rotated in the Gulf of Suez. The major directions of these fault systems are: clysmic trend, the most significant trend (310°–340°); the N oblique (350°–360° and 15°–30°); NW oblique trend (290°–300°); and the last one the cross trend (50°–75°). It was proposed that these fault trends are likely to have developed through the reactivation of preexisting fabrics (Patton et al. 1994).

From the surface data (Moustafa 1995), it is generally conceded that faults found in the northern and central sectors of the Gulf of Suez Rift showed pure normal offset along the NW–SE trend as well as oblique displacement. This indicate normal dip–slip component in addition to right or left lateral strike–slip components on the other fault trends. The right lateral strike–slip components characterize also some of the NW–SE- and WNW–ESE-oriented faults, whereas right and left lateral strike–slips characterize some of the NNE–SSW-oriented faults.

1.2 Focal mechanism data

The procedure of data analysis for estimating the parameters related to active crustal deformation (strain rate, velocities) is applied here (Kostrov 1974). This method is applicable to observational period of only 13 years according to the available data. The method of analysis based upon the knowledge of both fault planes of the focal mechanism solutions (strike, dip and slip) and seismic moment for each earthquake of data set. The

individual solutions of the focal mechanisms for 17 events provided by different sources in both central and northern sectors of the Gulf of Suez and recorded between 1992 and 2004 were used for estimating the seismic strain rate. The local magnitudes of these events range from 2.8 to 4.7. The mechanism solutions of ten events (Abu Elenean and Hussein 2007) were determined using the program Focmec (Snoke 2003) from *P*-wave first motion, S_V, and S_H first motion and amplitude ratios S_V/S_H, S_H/P and S_V/P of earthquakes before recorded digitally by Egyptian National Seismological Network (ENSN, Fig. 2). Figure 2 demonstrates the distribution of Egyptian National Seismological Network stations (ENSN) that improved the detection of earthquakes and increase the reliability of focal mechanism solutions even for small events. Morsy et al. (2011) constructed the mechanism of the last two events (16 and 17, Table 1) by the same way. Morsy et al. (2011) also used the same software to recalculate the first motion focal mechanism solutions for the events (1–5, Table 1) to obtain finer results. The first motion polarity readings of these events were collected from different sources (Maamoun 1985; Abu Elenean 1997; Abu Elenean and Hussein 2007; Megahed 2004; Abu Elenean et al. 2004). The focal mechanisms reflect a homogenization of the structural components; most events indicate pure dip–slip normal faulting mechanisms and dip–slip normal faulting with a strike–slip component (Table 1 and Fig. 2). Only few events show pure strike–slip faulting. The NW-, WNW-, NNE- and ENE-oriented nodal planes are quite concordant with the surface tectonics in the northern

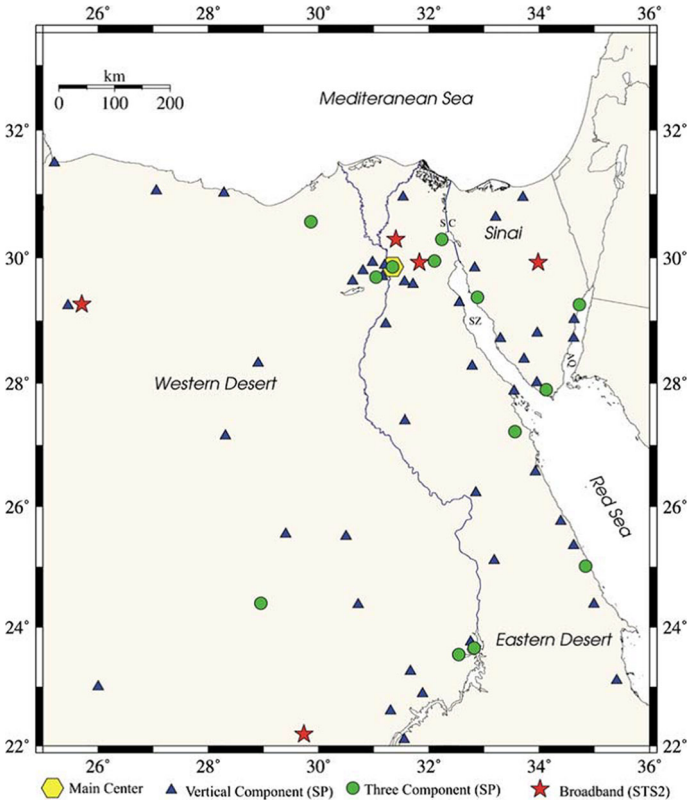

Fig. 2 Geographic distribution of the Egyptian National Seismic Network (ENSN). *AQ* Gulf of Aqaba, *SC* Suez Canal, *SZ* Gulf of Suez

Table 1 List of focal mechanism parameters for earthquakes in the northern/central parts of the Gulf of Suez used that were used in the moment tensor summation

No.	Date Y M D	OT H M S	Lat. N°	Long. E°	*h* (km)	ML	Strike°	Dip°	Rake°	REF
1	19921020	015758	28.510	33.160	10	3.8	262	40	− 162	M
2	19921027	090446	28.840	33.110	10	3.5	154	38	− 78	M
3	19921027	110247	28.780	33.180	17	4.2	155	57	− 66	M
4	19950908	121322	29.700	32.230	13	4.0	167	62	− 69	M
5	19960915	051811	28.254	33.604	06	4.3	358	23	− 35	M
6	20000509	184332	28.550	33.120	07	3.1	311	80	− 23	A
7	20000625	191848	28.210	33.480	18	4.6	131	52	− 51	A
8	20001103	211903	28.930	32.840	23	3.5	119	46	− 76	A
9	20010105	190037	28.670	33.160	12	3.4	167	57	− 66	A
10	20030115	113128	28.920	32.630	05	3.2	318	55	− 84	A
11	20030401	153442	28.510	32.880	7.5	3.2	155	27	− 67	A
12	20030403	051843	29.130	32.770	12	2.8	182	44	− 22	A
13	20030422	200253	28.990	32.750	14	3.3	174	66	− 51	A
14	20030909	083900	28.920	32.740	14	3.1	116	56	− 53	A
15	20030911	151433	29.820	32.350	04	3.1	339	48	− 31	A
16	20040706	121351	29.500	32.530	25	3.5	322	52	− 71	M
17	20040816	224250	28.940	32.780	07	3.2	182	75	− 4	M

Date (year month day); OT (H M S): origin time (hour minute second)

Lat. N° latitude

Long. E° longitude

H (km) depth; ML: local magnitude

Strike° (φ); dip (δ); rake° (λ)

Morsy et al. (2011) and Abu Elenean and Hussein (2007)

and central sectors of the gulf (Fig. 3). The depth range for the majority of the events is 4–14 km, and a few of them reflect relatively larger depths. Morsy et al. (2011) returned these unexpected depths to the uncertainty in the velocity model and the type of seismic phase to be used. The first five events in Table 1 were located by International Seismological Data Center (ISC). The uncertainty of their locations cannot exceed 5 km. The last events were located by Egyptian National Seismological Network (ENSN) with errors not exceed 4 km.

The focal mechanism solutions used in this article is assigned quality A (good) as it includes only events with at least eight polarity observations, the maximum gap is less than 90° and the standard error difference of strike, dip and rake is less than 20° as introduced by Reasenberg and Oppenheimer (1985).

1.3 Methodology

The magnitude of deformation is calculated in this study through the summation of seismic moment release and the shape of deformation in terms of representative focal mechanism tensor using the formula of Kostrov (1974) as follows:

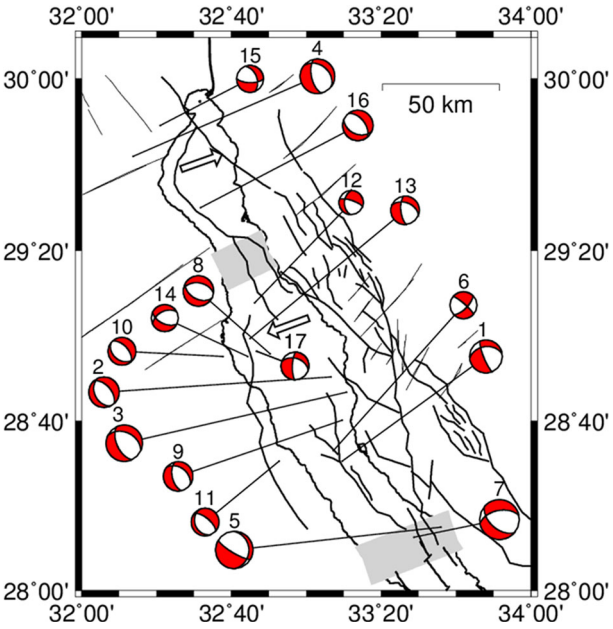

Fig. 3 Map showing the focal mechanism solutions; for the number for each solution, refer to Table 1

$$\acute{\epsilon}_{ij} = \frac{1}{2\mu VT}\sum_{n=1}^{N} Mij^{n}, \tag{1}$$

where μ is the shear modulus, V is the volume of the seismogenic layer, T is the time period of the earthquake record and m_{ij} is the unit moment tensor of the seismic moment of the nth earthquake determined from focal mechanism parameters. The above formula shows the linear proportionality of the average irrotational strain rate of a seismogenic layer of volume V resulting from earthquake dislocations with the sum of seismic moment tensors of all earthquakes occurring in that volume in time T. When the strike, dip and rake of the fault are known in addition to the scalar value of seismic moment (M_o), the geometrical moment tensor Mij for a shear dislocation can be completely described as

$$M_{ij} = M_o\left(b_i n_j + b_j n_i\right) \tag{2}$$

where M_o is the scalar moment and b and n are the unite vector in the direction of slip and the normal to the fault plane, respectively. Since the scalar seismic moment of the earthquakes used in this study were not available, we used the two calibrated scaling relations between the logarithm of moment and local magnitude constructed by Hussein et al. (2008) in order to calculate the scalar seismic moment of each earthquake from the conversion of M_L for the magnitude range $1.7 \leq M_L \leq 3.4$ and $3.5 \leq M_L \leq 6.7$, respectively.

$$\log M_0 = (1.0 \pm 0.05)M_L + (17.8 \pm 0.13) \tag{3A}$$

$$\log M_0 = (1.35 \pm 0.11)M_L + (16.3 \pm 0.53) \tag{3B}$$

where the moment magnitude *Mw* uncertainty in this equation is 0.3 (Hussein et al. 2008).

Following the coordinate system introduced in Aki and Richards (1980b), the fault slip is:

$$b = \begin{vmatrix} \cos\lambda\cos\varphi + \cos\delta\sin\lambda\sin\varphi \\ \cos\lambda\sin\varphi - \cos\delta\sin\lambda\cos\varphi \\ -\sin\lambda\sin\delta \end{vmatrix} \tag{4}$$

and normal to the fault plane is:

$$n = \begin{vmatrix} -\sin\varphi\sin\delta \\ \cos\varphi\sin\delta \\ \cos\delta \end{vmatrix} \tag{5}$$

where φ, δ and λ are the strike, dip and rake angle of the fault plane in degrees, respectively.

Using Eqs. 2–4, the elements of the symmetric moment tensor M_{ij} can be written as:

$$M_{11} = -(\sin\delta\cos\lambda\sin 2\varphi + \sin 2\delta\sin\lambda\sin^2\varphi)M_0 \tag{6}$$

$$M_{12} = -(\sin\delta\cos\lambda\cos 2\varphi + (1/2)\sin 2\delta\sin\lambda\sin 2\varphi)M_0 = M_{21} \tag{7}$$

$$M_{13} = (\cos\delta\cos\lambda\cos\varphi + \cos 2\delta\sin\lambda\sin\varphi)M_0 = M_{31} \tag{8}$$

$$M_{22} = (\sin\delta\cos\lambda\cos 2\varphi - \sin 2\delta\sin\lambda\cos^2\varphi)M_0 \tag{9}$$

$$M_{23} = -(\cos\delta\cos\lambda\sin\varphi + \cos 2\delta\sin\lambda\cos\varphi)M_0 = M_{32} \tag{10}$$

$$M_{33} = -(\sin 2\delta\sin\lambda)M_0 \tag{11}$$

where the subscripts 1, 2 and 3 are, respectively, correspond with north, east and vertically downward.

Using Eqs. 3A, 3B, 6–11, we estimate the elements of the symmetric moment tensor M_{ij} (Table 2).

Then by considering the area of study as a rectangular deforming region of length, width and thickness and using the formulation established by Jackson and Mckenzie (1988), we can calculate the elements of the velocity tensor, *Uij,* as follows:

$$\begin{aligned} u_{11} &= \frac{1}{2\mu l_2 l_3 T}\sum_{n=1}^{N} M_{11}^n, \quad u_{22} = \frac{1}{2\mu l_1 l_3 T}\sum_{n=1}^{N} M_{22}^n \quad u_{33} = \frac{1}{2\mu l_1 l_2 T}\sum_{n=1}^{N} M_{33}^n, \\ u_{13} &= \frac{1}{\mu l_1 l_3 T}\sum_{n=1}^{N} M_{13}^n, \quad u_{23} = \frac{1}{\mu l_1 l_3 T}\sum_{n=1}^{N} M_{23}^n, \quad u_{12} = \frac{1}{\mu l_1 l_2 T}\sum_{n=1}^{N} M_{12}^n \end{aligned} \tag{12}$$

where l_1 and l_2 denote the length and width of the deforming volume, respectively, and l_3 denote the thickness of the seismogenic layer.

2 Results

The elements of seismic strain tensor $\dot{\varepsilon}_{ij}$ within the central/northern parts of Gulf of Suez are deduced from the moment tensor summation following the above-mentioned method. The cumulative seismic moment release from 17 earthquakes over the 13 years (Table 2)

Table 2 Elements of moment tensor calculated from the parameters of fault plane solutions and scalar seismic moment of the earthquakes during the time period from 1992 to 2004

No.	ML	Log Mo	$M_0 \times 10^{22}$ dyn cm	$M_{33} \times 10^{22}$	$M_{11} \times 10^{22}$	$M_{22} \times 10^{22}$	$M_{13} \times 10^{22}$	$M_{23} \times 10^{22}$	$M_{12} \times 10^{22}$
1	3.8	21.43	2.69E–01	− 8.07E–02	1.27E–01	− 4.31E–02	− 4.04E–02	− 1.91E–01	1.48E–01
2	3.5	21.025	1.06E–01	− 1.01E–01	2.97E–02	7.10E–02	2.65E–02	1.48E–02	4.77E–02
3	4.2	21.97	9.33E–01	− 7.75E–01	3.83E–01	3.92E–01	3.73E–02	− 4.01E–01	5.04E–01
4	4	21.7	5.01E–01	− 3.86E–01	9.02E–02	3.01E–01	2.51E–02	− 2.76E–01	2.26E–01
5	4.3	22.105	1.27E+00	− 5.22E–01	2.55E–02	4.97E–01	− 9.81E–01	− 4.71E–01	4.20E–01
6	3.1	20.9	7.94E–02	− 1.03E–02	7.70E–02	− 6.67E–02	1.35E–02	2.86E–02	− 4.77E–02
7	4.6	22.51	3.24E+00	− 2.43E+00	2.98E+00	− 5.50E–01	3.56E–01	− 1.36E+00	9.71E–01
8	3.5	21.025	1.06E–01	− 1.03E–01	9.43E–02	8.47E–03	5.30E–03	− 1.69E–02	3.39E–02
9	3.4	21.2	1.58E–01	− 3.65E–02	3.01E–02	1.01E–01	2.06E–02	− 6.50E–02	7.77E–02
10	3.2	21	1.00E–01	− 9.50E–02	5.00E–02	4.30E–02	1.80E–02	2.90E–02	4.70E–02
11	3.2	21	1.00E–01	− 7.40E–02	2.70E–02	4.80E–02	5.40E–02	3.40E–02	4.80E–02
12	2.8	20.6	3.98E–02	− 1.47E–02	− 1.59E–03	1.67E–02	2.67E–02	1.59E–03	2.51E–02
13	3.3	21.1	1.26E–01	− 7.30E–02	1.64E–02	5.67E–02	2.52E–02	− 6.80E–02	7.81E–02
14	3.1	20.9	7.94E–02	− 5.88E–02	7.86E–02	− 1.99E–02	− 9.53E–03	− 3.42E–02	− 1.59E–03
15	3.1	20.9	7.94E–02	− 4.05E–02	3.89E–02	1.59E–03	− 4.13E–02	2.07E–02	5.08E–02
16	3.5	21.025	1.06E–01	− 9.75E–02	6.36E–02	3.39E–02	− 2.12E–03	3.18E–02	5.40E–02
17	3.2	21	1.00E–01	− 3.70E–02	− 4.00E–03	4.20E–02	2.00E–02	− 6.40E–02	6.30E–02
Cumulative seismic moment tensor *Mij* =			7.39E+00	− 4.93E+00	4.10E+00	9.32E–01	− 4.46E–01	− 2.79E+00	2.79E+00

is about 7.39 × 10^{22} dyne cm/year. The cumulative seismic moment tensor representative for this zone is

$$Mij = \begin{vmatrix} 4.100 & 2.790 & -0.446 \\ 2.790 & 0.930 & -2.790 \\ -0.446 & -2.790 & -4.930 \end{vmatrix} \times 10^{22} \text{ dyne cm} \quad (13)$$

To examine the degree of consistency between individual fault plane solutions, the normalized focal mechanism tensor is obtained by dividing all the elements of moment tensor summation ΣMij by the scalar seismic moment Mo of the nth focal mechanisms using the following equation:

$$Fij = \frac{\sum_{n=1}^{N} Mo^n mij^n}{\sum_{n=1}^{N} Mo^n} \quad (14)$$

where mij^n is a function only of the strike, dip and rake of the focal mechanism for a number of earthquakes (Aki and Richards 1980a), N is the number of all the focal mechanisms available and Mo^n is the corresponding scalar moment of the nth focal mechanisms. The obtained representative focal mechanism tensor F_{ij} for the study area is

$$F_{ij} = \begin{vmatrix} 0.55 & 0.37 & -0.06 \\ 0.37 & 0.12 & -0.37 \\ -0.06 & -0.37 & -0.66 \end{vmatrix} \quad (15)$$

The corresponding eigenvalues are

λ	Azimuth°	plunge°
0.8	33.1	9.78
0.01	143	21
− 0.81	279.5	66.69

The eigensystem of the F_{ij} indicates that the values of P (− 0.81), B (0.01) and T (0.8) axes are greatly close to − 1, 0, and 1, respectively, reflecting a homogeneity of data. This means that the focal mechanism solutions in this zone are similar.

Following the relations described earlier in this paper, the strain rate and velocity tensor are estimated for this zone. For these calculations, the deforming volume of the seismic zone is needed. The total dimension of the deformed volume obtained from the seismicity and tectonics of northern/central Gulf of Suez in the N–S and E–W directions is about 183 and 66.7 km, respectively. The thickness of the seismogenic layer was assumed to be 13 km, and the shear modulus μ is 3 × 10^{11} dyne cm. Using all the source mechanism solutions and the seismic moment values given in Table 2, the following strain tensor and velocity tensor are obtained using Eqs. 1 and 12 for the time span of 1992–2004 (T = 13 years).

$$\acute{\epsilon}_{ij} = \begin{vmatrix} 0.033 & 0.022 & -0.0036 \\ 0.022 & 0.0075 & -0.022 \\ -0.0036 & -0.022 & -0.039 \end{vmatrix} \times 10^{-9}/\text{year} \quad (16)$$

The sum of moment tensor suggests a T axis at N33.16°E with a plunge of 9.8° and a P axis at N279.46°E with a plunge of 66. 74°. These results correspond to a focal mechanism with a strike of 320.69°, a dip of 58° and a rake of − 65.17° (Fig. 4).

We also quantify the uncertainty due to the short period of observations using the definition of the variance after Shen-Tu et al. (1998), in which the moment tensor $M_o m_{ij}$ of each earthquake makes a contribution of $\pm M_o m_{ij}$ to the uncertainties in the strain rates. This measure of uncertainty will be used when we test for the reliability of self-similarity of data sample. When applying this definition on the present study, it yields small standard errors in the strain rate relative to the total magnitude of seismic strain rate of that area. This reveals that the used earthquake data set has fairly equal moment tensors.

$$\text{var}\,\epsilon ij = \sum \left(\frac{Momij}{2\mu VT}\right)^2 = \begin{vmatrix} 5.9 & 0.96 & 0.82 \\ 0.96 & 0.54 & 1.55 \\ 0.72 & 1.55 & 4.57 \end{vmatrix} \times 10^{-22} \tag{17}$$

The strain rate of this zone is about 0.045×10^{-9}/year. This low level of strain rate indicates that little seismic deformation has been occurred in this zone, which is also expected for small- and moderate-sized events.

The velocity tensor in the same coordination system is as follows:

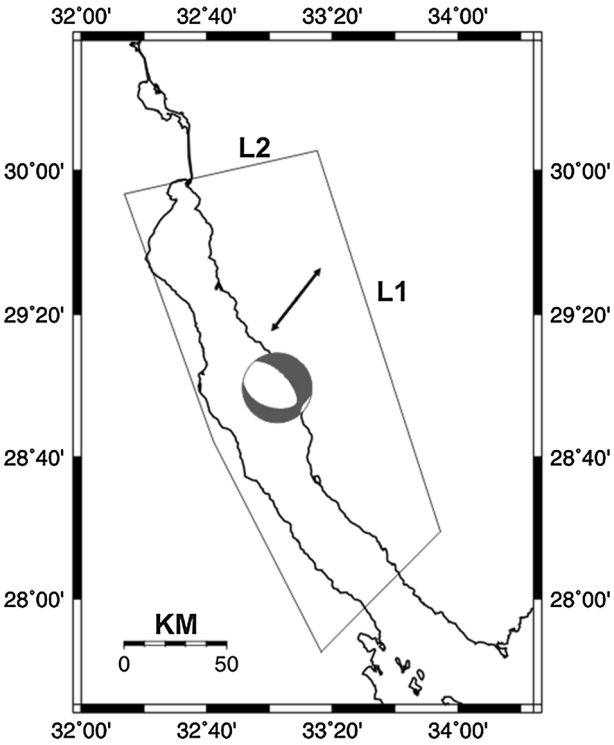

Fig. 4 Fault plane solution obtained from moment tensor summation; L1 and L2 denote the length and width of the seismogenic zone, respectively, and the outward arrows indicate the direction of the principal extensional strain axes

$$Uij = \begin{vmatrix} 6 & 3 & -0.48 \\ 3 & 0.50 & -3 \\ -0.48 & -3 & -0.517 \end{vmatrix} \times 10^{-3} \text{ mm/year} \quad (18)$$

In our case, as the length l_1 of the seismogenic layer is much greater than its width l_2, the horizontal shear velocity U_{12} of Eq. 18 is estimated from the following formula $u_{12} = \frac{1}{\mu l_1 l_3 T} \sum_{n=1}^{N} M_{12}^n$ instead of Eq. 4 (Jackson and Mckenzie 1988; Megahed 2004); the difference between the two expressions is that we divide by the thickness l_3 instead of the width l_2 of the volume deformed in Eq. 4.

The eigenvalues of the velocity tensor *Uij* are:

λ (m/year)	Azimuth°	Plunge°
− 0.0034	285	44.4
0.0017	129.4	42.93
0.0077	27.5	12.46

The results indicate that the dominant components of the strain tensor are $\dot{\varepsilon}_{33}$, $\dot{\varepsilon}_{11}$ and $\dot{\varepsilon}_{21}$, respectively. The dominant negative component $\dot{\varepsilon}_{33} = -0.039 \times 10^{-9}$/year reveals thinning of the seismogenic layer which is consistent with the normal faulting mechanism. The $\dot{\varepsilon}_{11} = 0.033 \times 10^{-9}$/year indicates N–S extension, while the positive $\dot{\varepsilon}_{21}$ component shows a right lateral shear component along E–W direction. Furthermore, the eigensystem of velocity tensor suggests that the deformation in the area of study is taken up mainly by extension in N28.0° direction at a rate of 0.008 ± 0.9e–08 mm/year and a vertical motion at a rate of 0.0034 ± 0.25e–08 mm/year expressed as a crustal thinning. The plunge of eigenvector representing the tension axis is very small reflecting a horizontal velocity.

3 Discussion and conclusions

Seismic moment summation is useful in understanding the contribution of seismic activity to the overall deformation in northern–central parts of the Gulf of Suez. From the seismic point of view, the new tectonic activity of this zone is witnessed by the occurrence of earthquakes. The northern/central Gulf of Suez can be considered as a moderate seismicity zone which is characterized by relatively small earthquakes ($M < 5$), mostly associated with the extensional processes along the NW–SE striking fault system. The present-day earthquake activity in the northern/central Gulf of Suez is closely connected to its tectonic history. Megahed (1987) reported that the abundant of basalt flows in the northern zone of the Suez Gulf and their position between the underlying Paleogene and overlying Neogene is likely to indicate the beginning of the renewed founding of the Gulf. This means that earthquake activity is mainly related to the history of the basement tectonics.

The present study mainly focuses on the fault plane solutions, with the main target of detecting a possible trend of deformation field through the analysis of the strain tensor during the period of investigation. A total number of 17 fault plane solutions were utilized to estimate the seismic strain tensor orientations in the study area using the Kostrov (1974) formula. The scalar seismic moment is estimated from earthquake magnitudes via the regression relations of Hussein et al. (2008). A combination of fault plane solutions and the

scalar seismic moment described the double couple moment tensor. Then, a linear combination of seismic moment tensors provides an indicative of average strain within a volume of interest. Although the available mechanisms represent small earthquakes ($2.8 \leq ML \leq 4.7$), their agreement appears to reflect the attribute of a regional stress field. The total moment released by the earthquakes analyzed in this study is equal to 7.39×10^{22} dyne cm. The main seismic deformation is extensional in the NE–SW direction (28°). This result is in a good agreement with the regional extension. The rate of extension is considerably small (8e–3 ± 0.9e–08 mm/year) along the NNE direction. The average seismotectonic strain rate is 0.045×10^{-9}/year. The normal mechanisms for events in the seismogenic layer of this seismic zone cause a negative $\dot{\varepsilon}_{33}$ and positive $\dot{\varepsilon}_{11}$. This means that there is a thinning of the seismogenic layer at a rate of 0.0034 ± 0.25e–08 mm/year. Based on the neotectonic studies (e.g., Steckler et al. 1988), the rate of thinning suggested here seems to be very small. This expected result is mainly related to the period of study which is too short relative to the geological ages. This area is also under going NE–SW extension, further supporting the separation of African and Arabian plates. The insufficient coverage of the recording stations before 1981 limited the number of fault plane solutions. The number of working stations in Egypt began to increase after 1981, and consequently, the reported data have increased gradually. Moreover, the dense distribution of Egyptian National Seismological Network stations (ENSN) from the beginning of 1998 improved the detection of small earthquakes and allows focal mechanism solutions for small events to be determined with a large number of P-wave polarity data. Due to the above reason, the strain tensor analysis is only applicable to a limited observational period of 13 years, which in fact requires a much longer observation period. Therefore, seismicity and focal mechanism will be updated gradually for obtaining more information for future studies.

A comparison between the results of the present study and that of Morsy et al. (2011) confirmed that the strength of the crust is uniform. This means a good correspondence between the principal stress and strain orientations, suggesting that this seismotectonic zone seems to be characterized by relatively homogeneous tectonic fabrics. The general trend of extensional strain axis direction N28°E shows a good correlation with similar results obtained from other investigations in the area (e.g., Morsy et al. 2011) and the Red Sea as deuced from the stress tensor (Delvaux and Barth 2010). The geodetic deformation derived from the analysis of GPS measurements in the area surrounding the Gulf of Suez (El-Fiky 2005) and within central part of the Gulf (Abdel-Monem et al. 2011) is well identical in style and direction with our results, while the rate of deformation is not the same. For example, it is seen that the dominant components of strain gradient are very small compared with those of GPS results. The extensional and compressional strain calculated here is 0.039e–09 and 0.033e–09, respectively, which is greatly less than those deduced from GPS data by Abdel-Monem et al. (2011) for the central zone of the Gulf. Their estimated values are 5.2e–07 and 0.134e–07 for extensional and compressional strain rate, respectively. Furthermore, this study indicates that the northern part of Gulf of Suez is still reflecting a small rate of crustal deformation (0.008 and 0.0034 mm/year of extension and thinning, respectively) which is about 6 times less than the southern part (0.05 and 0.03 mm/year, Megahed 2004) and 125 times less than the rate of extensional in the Gulf of Suez deduced from the geological information (< 1 mm/year, Steckler et al. 1988). This difference in rate between geological and seismic strain is mainly due to the fact that the seismotectonic deformation is relatively small compared to the total value of deformation in this seismogenic zone. This result confirms the view of Amelung and King (1997) that

the deformation direction due to small earthquakes is identical to the applied regional deformation, but their amplitudes can be different.

However, our results show a clockwise rotation to a more northerly direction of tension axis with respect to the N52°–56°E tension axis of Megahed (2004) and Abu Elenean (1997) in the southern part of the Gulf of Suez.

In accordance with the regional extensional forces acting along the Gulf of Suez, the earthquake activity and the obtained strain pattern in this zone are considered to be a direct consequence of the relative motions of African plate, Sinai and Arabia. Reilinger et al. (2006).

References

Abdel-Monem N, Abou Aly N, Mahmoud S, Shereif R, Salah M, Khalil H, Hassib GH, Rayan A (2011) GPS measurements of current crustal movements along the Gulf of Suez. In: NRIAG journal of geophysics special issue of the 2nd Arab conference on astronomy and geophysics, pp 45–66

Abu El-Nader I (2009) Seismotectonics of Egypt in view of an updated earthquake Catalogue. Ph.D. Thesis, Faculty of Science, Geology Department Mansoura University, Egypt

Abu Elenean KM (1997) A study on the seismotectonic of Egypt in relation to the Mediterranean and Red Seas tectonics. Ph.D. thesis, Faculty of Science, Ain Shams University, Cairo, Egypt

Abu Elenean KM, Hussein HM (2007) Source mechanism and source parameters of May 28, 1998 earthquake, Egypt. J Seismol 11:259–274

Abu Elenean K, Arvidsson R, Kulhanek O (2004) Focal mechanism of smaller earthquakes close to VBB Kottamia station, Egypt. Ann Geol Surv Egypt V(XXVII):357–368

Aki K, Richards P (1980a) Quantitative seismology. W.H. Freeman and Company, San Francisco, p 117

Aki K, Richards P (1980b) Quantitative seismology: theory and methods. Freemen Co, San Francisco, 557 pp

Amelung F (1996) Kinematics of small earthquakes and active tectonic and topography in the San Francisco Bay region. Ph.D. thesis

Amelung F, King G (1997) Large scale tectonic deformation inferred from small earthquakes. Nature 386:702–705

Amer R, Sultan M, Ripperdan R, Encarnacion J (2012) Structural architecture for development of marginal extensional sub-basins in the Red Sea active rift zone. Int J Geosci 3:133–152

Bosworth W (1985) Geometry of propagating continental rifts. Nature 316:625–627

Bosworth W (1995) A high- strain rift model for the southern Gulf of Suez (Egypt). In: Lambiase JJ (ed) Hydrocarbon habitat in rift basins, vol 80. Geological Society Special Publications, London, pp 75–112

Bosworth W, McClay KR (2001) Structural and stratigraphic evolution of the Gulf of Suez Rift, Egypt, a synthesis. In: Ziegler PA, Cavazza W, Robertson AHF, Crasquin-Soleau S (eds) Peri-tethys memoir 6: peri-tethyan rift/wrench basins and passive margins, vol 186. Memories du Museum National D'Histoire Naturelle, pp 567–606

Daggett P, Morgan P, Boulos FK, Hennin SF, el Sherif AA, El Sayed AA, Basta NZ, Melek YS (1986) Seismicity and active tectonics of the Egyptian Red Sea margin and the northern Red Sea margin and the northern Red Sea. Tectonophysics 125:313–324

Delvaux D, Barth A (2010) African stress pattern from formal inversion of focal mechanism data. Tectonophysics 482:105–128

Ekstrom G, England P (1989) Seismic strain rates in regions of distributed continental deformation. J Geophys Res 94:10231–10257

El-Fiky G (2005) GPS-derived velocity and crustal strain field in the Suez-Sinai Area, Egypt. Bull Earthq Res Inst Univ Tokyo 2:1–20

Garfunkel Z, Ben-Avraham Z (1996) The structure of the dead sea basin. Tectonophysics 266(1–4):155–176

Hussein HM, Marzouk I, Moustafa AR, Hurukawa N (2006) Preliminary seismicity and focal mechanisms in the southern Gulf of Suez: August 1994 through December 1997. J Afr Earth Sci 45:48–60

Hussein HM, Abu Elenean KM, Marzouk IA, Peresan A, Korrat IM, Abu El-Nader E, Panza GF, El-Gabry MN (2008) Integration and magnitude homogenization of the Egyptian earthquake catalogue. Nat Hazards 47:525–546

Jackson J, McKenzie D (1988) The relationship between plate motions and seismic moment tensors, and the rates of active deformation in the Mediterranean and Middle East. J Geophys 93:45–73
Kostrov V (1974) Seismic moment and energy of earthquakes, and seismic row of rock. Izv Acad Sci USSR Phys Solid Earth 1:23–44
Kulhanek O, Korrat I, El Sayed A (1992) Connection of the seismicity in the Red Sea and Egypt. Published abstract in the 10th annual meeting of the Egyptian geophysical society, 1–3 March 1992
Lyberis N (1988) Tectonic evolution of the Gulf of Aqaba. Tectonophysics 153:209–220
Maamoun M (1985) Shukeir earthquake June 12 th., 1983, Gulf of Suez, Egypt: Radiation pattern of first motion and its tectonic implication. Hiag V(B):161–173
Maamoun M, Megahed A, Allam A (1984) Seismicity of Egypt. HIAG Bull IV(B):109–160
McClusky S, Reilinger R, Mahmoud S, Ben Sari D, Tealeb A (2003) GPS constraints on Africa (Nubia) and Arabia plate motions. J Geophys Int 155:126–138
Megahed A (1987) A study on geotectonics and seismic regionalization of Egypt. M.Sc. thesis, Faculty of Science, Al-Azhar University, Cairo, Egypt
Megahed A (2004) Seismic deformation studies on the northeastern part of Egypt. Ph.D. thesis, Faculty of Science, Geology Department, Mansoura University of Egypt
Moretti I, Colletta B (1987) Spatial and temporal evolution of the Suez rift: a combination of stretching and secondary convection. Tectonophysics 133:229–234
Morsy M, Hussein HM, Abou Elenean KM, El-Hady SH (2011) Stress field in the central and northern parts of the Gulf of Suez area, Egypt from earthquake fault plane solutions. J Afr Earth Sci 60:293–302
Moustafa AM (1976) Block faulting in the Gulf of Suez. Fifth E.G.P.C. Exploration Seminar, Cairo, pp 1–19
Moustafa AR (1995) Internal structure and deformation of an accommodation zone in the northern part of the Suez rift and Red Sea. J Struct Geol 18:93–107
Patton TL, Moustafa AR, Nelson RA, Abdine SA (1994) Tectonic evolution and structural setting of the Suez Rift. In: Landon SM (ed) Interior rift basins, vol 59. AAPG Memoir, Athens, pp 9–55
Reasenberg P, Oppenheimer D (1985) FPFIT, FPPLOT, and FPPAGE: FORTRAN computer programs for calculating and displaying earthquake fault-plane solutions. US Geol Surv Open-File Rep 109:85–739
Reilinger R, McClusky S, Vernant P, Lawrence S, Ergintav S, Cakmak R, Ozener H, Kadirov F, Guliev I, Stepanyan R, Nadariya M, Hahubia G, Mahmoud S, Sakr K, ArRajehi A, Paradissis D, Al-Aydrus A, Rilepin M, Guseva T, Evren E, Dmitrotsa A, Filikov SV, Gomez F, Al-Ghazzi R, Karam G (2006) GPS constraints on continental deformation in the Africa–Arabia–Eurasia continental collision zone and implications for the dynamics of plate interactions. J Geophys Res 111:1–26. https://doi.org/10.1029/2005jb004051
Said R (1962) The geology of Egypt. Elsevier, Amsterdam, p 377
Shen-Tu B, Holt WE, Haines AJ (1998) The contemporary kinematics of the western United States determined from earthquake moment tensors, very long baseline interferometry and GPS observations. J Geophys Res 103(18087–18):117
Snoke A (2003) Focal mechanism determination software (FOCMEC Package)
Steckler M, Berthelot F, Lyberis N, Le Pichon X (1988) Subsidence in the Gulf of Suez: implication for rifting and plate kinematics. Tectonophysics 153:249–270
Younes AI, McClay KR (2002) Development of accommodation zones in the Gulf of Suez-Red Sea rift, Egypt. AAPG Bull 86:1003–1026